

# Functional Mapping of Interacting Regions of the Photoreceptor Phosphodiesterase (PDE6) $\gamma$ -Subunit with PDE6 Catalytic Dimer, Transducin, and Regulator of G-protein Signaling 9–1 (RGS9–1)\*

Received for publication, April 30, 2012, and in revised form, May 30, 2012. Published, JBC Papers in Press, June 4, 2012, DOI 10.1074/jbc.M112.377333

Xiu-Jun Zhang, Xiong-Zhuo Gao, Wei Yao, and Rick H. Cote<sup>1</sup>

From the Department of Molecular, Cellular, and Biomedical Sciences, University of New Hampshire, Durham, New Hampshire 03824

**Background:** The PDE6  $\gamma$ -subunit serves multiple functions during visual transduction.

**Results:** Several regions of  $P\gamma$  that interact with PDE6 or transducin were identified.

**Conclusion:** Multiple interacting sites of  $P\gamma$  with PDE catalytic dimer, transducin, and the transducin/RGS9 complex coordinate the activation and deactivation of PDE6.

**Significance:** This work contributes to understanding how defects in PDE6 structure/function lead to retinal disease.

The cGMP phosphodiesterase (PDE6) involved in visual transduction in photoreceptor cells contains two inhibitory  $\gamma$ -subunits ( $P\gamma$ ) which bind to the catalytic core ( $P\alpha\beta$ ) to inhibit catalysis and stimulate cGMP binding to the GAF domains of  $P\alpha\beta$ . During visual excitation, interaction of activated transducin with  $P\gamma$  relieves inhibition.  $P\gamma$  also participates in a complex with RGS9–1 and other proteins to accelerate the GTPase activity of activated transducin. We studied the structural determinants for these important functions of  $P\gamma$ . First, we identified two important sites in the middle region of  $P\gamma$  (amino acids 27–38 and 52–54) that significantly stabilize the overall binding affinity of  $P\gamma$  with  $P\alpha\beta$ . The ability of  $P\gamma$  to stimulate noncatalytic cGMP binding to the GAF domains of PDE6 has been localized to amino acids 27–30 of  $P\gamma$ . Transducin activation of PDE6 catalysis critically depends on the presence of Ile54 in the glycine-rich region of  $P\gamma$  in order to relieve inhibition of catalysis. The central glycine-rich region of  $P\gamma$  is also required for transducin to increase cGMP exchange at the GAF domains. Finally, Thr-65 and/or Val-66 of  $P\gamma$  are critical residues for  $P\gamma$  to stimulate GTPase activity of transducin in a complex with RGS9–1. We propose that the glycine-rich region of  $P\gamma$  is a primary docking site for PDE6-interacting proteins involved in the activation/inactivation pathways of visual transduction. This functional mapping of  $P\gamma$  with its binding partners demonstrates the remarkable versatility of this multifunctional protein and its central role in regulating the activation and lifetime of visual transduction.

Rod and cone photoreceptors respond to light by triggering a biochemical cascade leading to the activation of the cGMP-

specific phosphodiesterase (PDE6).<sup>2</sup> Because of its dominant role in controlling cGMP levels (and hence membrane conductance), the extent and duration of PDE6 activation must be precisely regulated. Catalytic activity of the rod PDE6 catalytic heterodimer ( $P\alpha\beta$ ) is directly regulated by its inhibitory  $\gamma$ -subunits ( $P\gamma$ ) that tightly bind to  $P\alpha\beta$  to inhibit catalysis in the dark-adapted photoreceptor cell (1). During the first steps in vision, photoisomerized rhodopsin activates transducin, which binds GTP and releases its activated  $\alpha$ -subunit ( $T\alpha^*$ -GTP) to activate the PDE6 holoenzyme ( $\alpha\beta\gamma\gamma$ ) by relieving the inhibition by  $P\gamma$  at the active sites of the enzyme. The recovery of the dark-adapted state requires inactivation of  $T\alpha^*$ -GTP by its intrinsic GTPase activity which is the rate-limiting step for recovery of the photoresponse. The GTPase rate of  $T\alpha^*$ -GTP is modulated by the Regulator of G-protein Signaling 9–1 (RGS9–1) to which  $P\gamma$  binds to potentiate the GTPase-accelerating function of RGS9–1 (2). The importance of the proper functioning and regulation of these proteins is underscored by the fact that genetic disruptions of PDE6 or the proteins with which it interacts often result in a loss of visual function, photoreceptor degeneration, and/or blindness (3–5).

The 87-amino acid  $P\gamma$  subunit (localized to the signal-transducing outer segment compartment of rod photoreceptors) is remarkable for the variety of regulatory functions it performs as well as the multitude of proteins with which it interacts in addition to the catalytic subunits of PDE6 (6). The primary regulatory role of  $P\gamma$  is to regulate access of substrate to the catalytic pocket of PDE6 and thereby control cGMP hydrolytic rates. This function is carried out by the last few C-terminal residues of  $P\gamma$  interacting with the PDE6 catalytic domains in the immediate vicinity of the active site (7–9). An allosterically mediated inhibition of catalysis that occurs in the absence of the C-ter-

\* This work was supported, in whole or in part, by National Institutes of Health Grant EY-05798. Partial funding was provided by the New Hampshire Agricultural Experiment Station. This is Scientific Contribution Number 2479.

<sup>1</sup> To whom correspondence should be addressed: Department of Molecular, Cellular, and Biomedical Science, University of New Hampshire, Durham, NH 03824. Tel.: 603-862-2458; Fax: 603-862-4013; E-mail: rick.cote@unh.edu.

<sup>2</sup> The abbreviations used are: PDE, cyclic nucleotide phosphodiesterase; GTP $\gamma$ S, guanosine 5'-3-O-(thio)triphosphate;  $P\alpha\beta$ , catalytic dimer of PDE6  $\alpha$ - and  $\beta$ -subunits;  $P\gamma$ , inhibitory  $\gamma$  subunit of PDE6; GAF, regulatory domain of PDE6 named for their presence in cGMP-regulated PDEs, certain adenylate cyclases, and the transcription factor Fh1A of bacteria;  $T\alpha^*$ , activated transducin  $\alpha$ -subunit.

minal residues of P $\gamma$  has also been identified (10). P $\gamma$  also enhances the affinity with which cGMP binds to noncatalytic binding sites within the regulatory domain of the PDE6 catalytic dimer (11, 12); the region of P $\gamma$  responsible for this effect is in the central region of the P $\gamma$  sequence, which is known to have high affinity for the catalytic dimer (13–15). In addition to these two distinct functional regions, chemical cross-linking studies support the idea that P $\gamma$  binds in an extended conformation along the entire surface of the catalytic subunits (16, 17), including both regulatory domains (GAFa and GAFb, named for their widespread occurrence in cGMP PDEs, certain adenylylate cyclases, and the *Escherichia coli* Fh1a protein (18)) and the catalytic domains.

The molecular mechanism by which activated transducin  $\alpha$ -subunit interacts with P $\gamma$  to de-inhibit catalysis of the PDE6 holoenzyme is not well understood. Biochemical, structural, and physiological studies support a model in which T $\alpha^*$ -GTP binds not only to the C-terminal tail of P $\gamma$  (to displace P $\gamma$  from occluding the PDE6 catalytic pocket), but also to several additional sites (most notably Trp-70 and Leu-76) within the last third of the P $\gamma$  sequence (19–26). However, P $\alpha\beta$  reconstituted with P $\gamma$ 63–87 (*i.e.* the C-terminal fragment of P $\gamma$  consisting of amino acids 63 to 87) could not be activated by T $\alpha^*$ -GTP $\gamma$ S (10), indicating that additional sites of interaction of activated transducin with P $\gamma$  are required for activation of the PDE6 holoenzyme. The N-terminal half of P $\gamma$  (specifically amino acids 24–45) has been reported to interact with transducin  $\alpha$ -subunit (27–30), and the greater efficiency with which cone *versus* rod PDE6 can be activated by transducin has been attributed to differences in the GAF binding interactions with P $\gamma$  (31). However, cross-linking and pull-down experiments suggest that T $\alpha^*$ -GTP interactions are weaker with the N-terminal half of P $\gamma$  than with the C-terminal region (26), raising questions about the functional significance of these interactions.

The recovery of the dark-adapted state following cessation of a light stimulus requires the inactivation of T $\alpha$ -GTP by its intrinsic GTPase activity; this reaction has been shown to be rate-limiting for the recovery of the rod photoresponse (32). This GTPase rate is determined by a complex of proteins that include T $\alpha^*$ -GTP, RGS9–1, and other proteins (33); P $\gamma$  serves to facilitate the formation of a tighter complex of these proteins to potentiate the GTPase accelerating function of RGS9–1 (34–37). However, the interaction surface of P $\gamma$  with RGS9–1 and the functional significance of the interactions are unclear. Whereas biochemical and structural evidence shows that the C-terminal region of P $\gamma$  can bind to RGS9–1 (20, 23, 38), cross-linking and interaction assays have implicated the N-terminal half of P $\gamma$  in binding to the transducin/RGS9 complex (39). Furthermore, transgenic animals expressing a phosphorylation-incompetent mutation at Thr-35 of P $\gamma$  show altered photoresponse kinetics consistent with a disruption of the P $\gamma$ -mediated acceleration of GTPase activity by RGS9–1 (40).

In this report, we used functional interaction assays to demonstrate that the intrinsically disordered P $\gamma$  subunit forms multiple stabilizing interactions with P $\alpha\beta$  that extend from the N-terminal region of P $\gamma$  (interacting with the cGMP binding site in the GAFa domain) to the last several C-terminal residues of P $\gamma$  (serving to occlude the active site in the catalytic domain),

and including a newly discovered interaction region in the glycine-rich central portion of P $\gamma$ . We also localized the P $\gamma$  residues directly responsible enhancing the ability of cGMP to bind to the noncatalytic binding sites on the PDE6 catalytic dimer, and identified neighboring residues that stabilize this effect. Finally, we identified the structural requirements for P $\gamma$  to effectively interact with activated transducin to activate PDE6 catalysis (at the enzyme active site), to increase cGMP exchange (with noncatalytic binding sites in the regulatory GAFa domain), and to bind to the transducin/RGS9–1 complex (to accelerate the GTPase rate of the transducin  $\alpha$ -subunit). Together, these results provide a framework for understanding the sequential interactions of P $\gamma$  with PDE6 catalytic subunits and with its other binding partners that allow for precise temporal control of PDE activation and inactivation during visual transduction.

## EXPERIMENTAL PROCEDURES

**Materials**—Bovine retinas were purchased from W. L. Lawson, Inc. Synthetic peptides P $\gamma$ 10–30, P $\gamma$ 19–30, P $\gamma$ 21–30, P $\gamma$ 63–87, P $\gamma$ 65–87, and P $\gamma$ 68–87 were purchased from New England Peptide. Ultima Gold scintillation fluid was from PerkinElmer Life & Analytical Sciences. Filtration membranes were from Millipore, the bicinchoninic acid protein assay reagents and immobilized glutathione were from Thermo Scientific/Pierce. All other chemicals were from Sigma-Aldrich. [ $^3$ H]cGMP and [ $\gamma$ - $^{32}$ P]GTP were from PerkinElmer Life & Analytical Sciences. The primers for constructing P $\gamma$  mutants were obtained from Invitrogen. The plasmid purification kits were from Qiagen.

**Construction of P $\gamma$  Mutants**—Mutants lacking specific regions of the N-terminal sequence were constructed by PCR using primers designed to amplify various portions of the bovine rod P $\gamma$  sequence. The PCR products were inserted into the NotI and BamHI sites of pGEX-6P-1 vector, and followed by transformation into the *E. coli* BL21/(DE3) strain. The sequence of all P $\gamma$  mutants was confirmed by DNA sequencing at the Hubbard Center for Genome Studies (University of New Hampshire).

**Purification of P $\gamma$  Mutants**—Following expression of recombinant P $\gamma$  mutants in *E. coli* BL21(DE3), the bacterial extract was purified by immobilized glutathione. The affinity-purified protein was treated with HRV3C protease to remove the glutathione *S*-transferase fusion protein. Immobilized glutathione beads were added to the cleavage mix to remove any un-cleaved protein and the cleaved glutathione *S*-transferase. The P $\gamma$  mutants (containing five additional N-terminal amino acids derived from the fusion partner) were then further purified by C18 reverse-phase high pressure liquid chromatography. The purity (> 95%) and size of these proteins were evaluated by sodium dodecyl sulfate-polyacrylamide gel electrophoresis. Protein concentrations were determined by the bicinchoninic acid protein assay (41) using bovine  $\gamma$ -globulin as a standard. In those P $\gamma$  constructs that were directly compared (*e.g.* full-length P $\gamma$ , P $\gamma$ 67–87), we failed to observe an effect of the five additional N-terminal amino acids on P $\gamma$  inhibitory potency for P $\alpha\beta$ .

## Functional Interaction Sites of P $\gamma$ with PDE6 and Transducin

**PDE6 and P $\alpha\beta$  Purification and Functional Assays**—Bovine rod PDE6 was purified from bovine retinas as described (42). P $\alpha\beta$  catalytic dimers lacking P $\gamma$  were prepared by limited trypsin proteolysis and re-purified by Mono Q anion exchange chromatography prior to use (42). PDE6 catalytic activity was measured in 20 mM Tris, 10 mM MgCl<sub>2</sub>, 0.5 mg/ml bovine serum albumin, using a colorimetric assay (43). The PDE6 concentration was estimated based on the rate of cGMP hydrolysis of trypsin-activated PDE6 and the knowledge of the  $k_{\text{cat}}$  of the enzyme (5600 mol cGMP hydrolyzed per mol P $\alpha\beta$  per s (44)).

The inhibition potency (IC<sub>50</sub>) of synthetic peptides and P $\gamma$  truncation mutants was determined using 0.2 nM P $\alpha\beta$  and 2 mM cGMP as substrates. Under these conditions, wild-type P $\gamma$  and N-terminal mutants up to P $\gamma$ 21–87 inhibited P $\alpha\beta$  in a stoichiometric manner, behavior consistent with previous studies (44, 45).

[<sup>3</sup>H]cGMP binding to PDE6 was measured with a filter binding assay (46). The maximum binding of [<sup>3</sup>H]cGMP to nucleotide-depleted P $\alpha\beta$  was typically between 1 to 2 mol cGMP per mol P $\alpha\beta$  in the presence of wild-type P $\gamma$ . For measurements of cGMP dissociation kinetics, P $\alpha\beta$  reconstituted with P $\gamma$  or P $\gamma$  mutants were first incubated with 1  $\mu$ M [<sup>3</sup>H]cGMP for 5 min at room temperature, and at time 0 1 mM unlabeled cGMP was added, and samples were filtered at various times thereafter.

**Preparation of Bovine Rod Outer Segments (ROS) and GTPase Assay**—Bovine rod outer segment (ROS) were prepared from commercial frozen bovine retinas on a step sucrose gradient using the standard method under dark condition (42) and stored at –80 degree. GTPase activity of transducin was determined by a single-turnover technique described in Ref. 47. In brief, ROS membrane was washed with assay buffer in dark (10 mM Tris, pH 7.8, 100 mM NaCl, 8 mM MgCl<sub>2</sub>, 1 mM DTT), the pellet was exposed to light for 1 min and then re-suspended in assay buffer. The reaction was initiated by mixing 20  $\mu$ l of ROS membrane (20  $\mu$ M rhodopsin final concentration) and 20  $\mu$ l of 0.2  $\mu$ M [ $\gamma$ -<sup>32</sup>P]GTP. The reaction was stopped by addition of 100  $\mu$ l of 6% perchloric acid. [<sup>32</sup>P]P<sub>i</sub> was separated by activated charcoal and determined by liquid scintillation counting.

**Purification of Persistently Activated Transducin  $\alpha$ -Subunit (T $\alpha^*$ -GTP $\gamma$ S) and Transducin Activation of Reconstituted P $\alpha\beta$  and P $\gamma$  Mutants**—Transducin  $\alpha$ -subunits were extracted from the PDE6-depleted ROS membranes by addition of 50  $\mu$ M GTP $\gamma$ S. The extracted T $\alpha^*$ -GTP $\gamma$ S was purified on a Blue-Sepharose column as described (48, 49), followed by gel filtration chromatography to completely remove PDE6. The concentration of T $\alpha^*$ -GTP $\gamma$ S was determined by a colorimetric protein assay. Purified T $\alpha^*$ -GTP $\gamma$ S was stored at 4 °C and used within a few weeks. For the transducin activation measurement, purified P $\alpha\beta$  was pre-incubated with P $\gamma$  mutants or P $\gamma$  peptides at the indicated concentration to inhibit PDE activity (see figure legends). Ten micro molar-activated transducin (supplemented with 50  $\mu$ M GTP $\gamma$ S) was added to above mixture and incubated for 5 min. The PDE activity was measured using 2 mM cGMP as substrate.

**Data Analysis**—All experiments were repeated at least three times, and averages are reported as the mean  $\pm$  S.E. Curve fitting was performed using Sigmaplot (SPSS, Inc.).

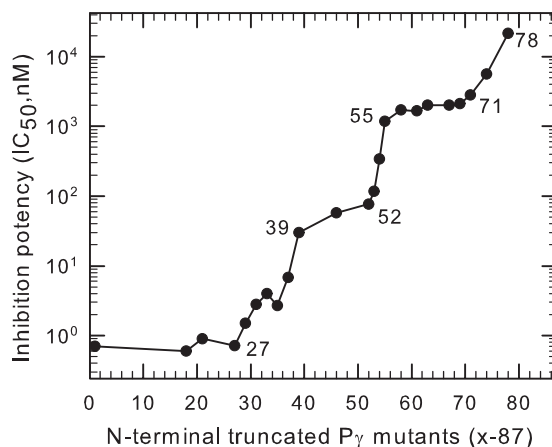


**FIGURE 1. Multiple regions of P $\gamma$  stabilize its interaction with PDE6 catalytic dimer to inhibit catalysis.** Purified P $\alpha\beta$  (0.2 nM) was pre-incubated with the indicated N-terminal truncated P $\gamma$  mutants (P $\gamma$ x-87) for 20 min, followed by addition of 2 mM cGMP substrate. Catalytic activity was measured by the phosphate release assay. The inhibition potency (IC<sub>50</sub>) was calculated from curve fitting the results to a 3-parameter logistic equation. The data represent the mean of at least three experiments; error bars (coefficient of variation < 10% in all cases) were omitted for clarity. The abscissa represents the position number of the starting amino acid of the N-terminal truncated P $\gamma$  mutant, with position 1 being the wild-type sequence. Data for P $\gamma$ 63–87, P $\gamma$ 71–87, P $\gamma$ 74–87, and P $\gamma$ 78–87 were taken from Ref. 10.

## RESULTS AND DISCUSSION

**Multiple Regions of P $\gamma$  Contribute to the High Affinity with Which P $\gamma$  Inhibits Catalysis**—Previous studies have defined two distinct regions of P $\gamma$  that interact with PDE6 catalytic dimer, but did not account for the very high affinity of P $\gamma$  for the PDE6 catalytic dimer (see Introduction). We hypothesized that P $\gamma$  must contain as-yet undiscovered interacting sites, which are responsible for stabilizing P $\gamma$  binding to P $\alpha\beta$ . To test this, we generated a series of N-terminal truncated P $\gamma$  mutants, all of which contain the last ten amino acids as a reporter of the ability to inhibit catalysis. By comparing the relative binding affinity of various N-terminal truncated peptides, we discovered two new interaction “hotspots” for P $\gamma$  with P $\alpha\beta$ . Fig. 1 shows that P $\gamma$  mutants lacking amino acid residues 27 to 38 showed a progressive, ~20-fold loss of binding affinity. A second region that stabilized P $\gamma$  binding to P $\alpha\beta$  by ~15-fold was identified as Asp52-Asp53-Ile54 within the glycine-rich region of P $\gamma$  (Fig. 1). (A third set of stabilizing residues (Leu78-His79-Glu80) was previously identified in the C-terminal region (10).) In contrast, amino acid residues 1–26, 39–51, and 55–62 of P $\gamma$  showed little ability to stabilize the inhibition of catalysis at the active site (Fig. 1). We conclude from this analysis that three discrete regions of the P $\gamma$  sequence (*i.e.* polycationic region, glycine-rich region, and C-terminal region) account for almost all of the favorable interactions that contribute to the high overall affinity of P $\gamma$  for the catalytic dimer of PDE6. An important physiological implication of these multiple P $\gamma$ -P $\alpha\beta$  stabilizing regions is that the P $\gamma$  subunit is very unlikely to interact with binding partners other than PDE6 in the dark-adapted state of the photoreceptor cell.

**The Ability of N-terminal P $\gamma$  Fragments to Augment Inhibition of Catalysis by the C-terminal Region of P $\gamma$** —Previously we reported that a P $\gamma$  truncation mutant lacking the last 17 amino acids at its C terminus (P $\gamma$ 1–70) enhanced 100-fold the ability

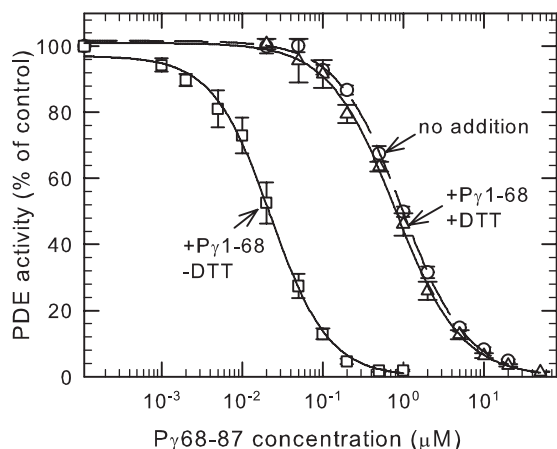


**FIGURE 2. An intermolecular disulfide bond between an N-terminal and C-terminal P $\gamma$  fragment enhances the inhibitory potency of the C-terminal region of P $\gamma$ .** Purified P $\alpha\beta$  (0.2 nM) was pre-incubated with 1  $\mu$ M P $\gamma$ 1–68 and increasing concentrations of P $\gamma$ 68–87 in the presence ( $\Delta$ ) or absence ( $\square$ ) of 1 mM DTT. The concentration dependence of P $\gamma$ 68–87 was also assayed in the absence of P $\gamma$ 1–68 ( $\circ$ ). PDE catalytic activity was measured following addition of 2 mM cGMP. The data are the mean  $\pm$  S.E. ( $n = 4$ ). The lines represent the fit to a 3-parameter logistic equation with  $IC_{50}$  values of: P $\gamma$ 68–87 alone =  $1.0 \pm 0.03 \mu$ M; +P $\gamma$ 1–68 plus DTT =  $0.8 \pm 0.03 \mu$ M, and; +P $\gamma$ 1–68 minus DTT =  $0.02 \pm 0.001 \mu$ M.

of a synthetic peptide (P $\gamma$ 63–87) to inhibit catalysis; shorter truncation mutants (e.g. P $\gamma$ 1–60) or smaller C-terminal peptides failed to exhibit this effect (10). To pinpoint the amino acids of P $\gamma$  responsible for this effect, we constructed several synthetic peptides (P $\gamma$ 69–87, P $\gamma$ 68–87, and P $\gamma$ 67–87) and truncation mutants (P $\gamma$ 1–67 and P $\gamma$ 1–68). Testing various combinations of N-terminal and C-terminal fragments of P $\gamma$ , we found that P $\gamma$ 1–68 in combination with P $\gamma$ 68–87 was able to exhibit the same enhancement of inhibitory effectiveness as reported in the earlier study. This mixture of two P $\gamma$  fragments overlapping only at Cys-68 have an overall binding affinity ( $IC_{50} = 20$  nM; Fig. 2) that is 100-fold less than the value for wild-type P $\gamma$  under the same experimental conditions.

To study the importance of the Cys-68 residue that is shared by both P $\gamma$  fragments, we constructed site-directed mutants in which serine or alanine replacing the naturally occurring Cys-68 terminal residue in the P $\gamma$ 1–68 truncation mutant. We found that neither the P $\gamma$ 1–68Ser nor the P $\gamma$ 1–68Ala were able to enhance the effectiveness of the C-terminal P $\gamma$ 68–87 peptide to inhibit P $\alpha\beta$  (data not shown). This led us to carefully evaluate the possibility that disulfide bond formation between the two P $\gamma$  fragments might be responsible for the enhanced inhibitory potency when P $\gamma$ 1–68 and P $\gamma$ 68–87 were incubated with P $\alpha\beta$ . To test this, we compared the behavior of identical mixtures of P $\alpha\beta$  and the two P $\gamma$  fragments in the presence or absence of 1 mM DTT. As shown in Fig. 2, P $\gamma$ 1–68 failed to enhance the potency of P $\gamma$ 68–87 in the presence of DTT, indicating that disulfide bond formation between the two fragments was responsible for the enhancement of inhibitory potency. Control experiments confirmed that 1 mM DTT had no effects on the apparent inhibitory potency of P $\gamma$ 68–87 in the absence of the N-terminal P $\gamma$  fragment (data not shown). These results fail to support the idea that allosteric communication induced by the N-terminal fragment alters the conformation of the catalytic domain (10).

The ability of the N-terminal half of P $\gamma$  to enhance 50-fold the binding of P $\gamma$ 68–87 when the two fragments are tethered to each other by a disulfide bond implies that substantial conformational flexibility likely exists between different regions of P $\gamma$ . Under this artificial circumstance, the N-terminal region anchors P $\gamma$  to the catalytic subunit, and brings the C-terminal region into proximity of the active site to permit inhibition of catalysis. The fact that the overall effectiveness of inhibition is 100-fold less than the wild-type protein implies that disruption of the local structure of P $\gamma$  caused by linking the two fragments by a disulfide bond impairs the ability of the C-terminal inhibitory residues to bind to the active site of the enzyme.

**Important P $\gamma$  Interaction Sites with P $\alpha\beta$  to Enhance cGMP Binding to the GAF Domain of PDE6—**Having identified the important interacting residues of P $\gamma$  with PDE6 catalytic dimer to increase the inhibition potency, we next questioned to what extent these interaction sites contributed to the ability of P $\gamma$  to stabilize cGMP binding to the GAF domains of PDE6. To test this, we first measured the ability of a series of N-terminal truncated mutations to stabilize cGMP binding to the GAF domain of P $\alpha\beta$ . As shown in Fig. 3A, P $\gamma$ 18–87 and P $\gamma$ 21–87 were able to stimulate cGMP binding to the same extent as wild type P $\gamma$  and with a similar binding affinity ( $K_{1/2} = 30$ –50 nM). Although the P $\gamma$ 27–87 mutant was able to stimulate cGMP binding to P $\alpha\beta$  to the same maximum extent as wild type P $\gamma$ , the affinity was reduced 7-fold compared with P $\gamma$ 21–87 (Fig. 3A). Removing two additional residues (P $\gamma$ 29–87) reduced to one-half the maximum extent of stimulation of cGMP binding (Fig. 3A), while P $\gamma$ 31–87 was ineffective (<20% stimulation; data not shown). We conclude from these N-terminal P $\gamma$  truncation mutants that amino acids 27–30 of P $\gamma$  are required to maximally stimulate cGMP binding to the GAFa domains of PDE6. Furthermore, neighboring amino acids (amino acids 21 through 26) enhance the local interactions between P $\gamma$  and the GAFa domain of P $\alpha\beta$  that result in stimulation of cGMP binding.

To better define the region of P $\gamma$  responsible for stimulating cGMP binding to the GAFa domains of P $\alpha\beta$ , we resorted to using small synthetic peptides of this region of P $\gamma$ . Although the shortest peptide we tested, P $\gamma$ 21–30, contained the residues identified above as being important for stimulating cGMP binding (Fig. 3A), this 10-residue oligopeptide lacked sufficient affinity for P $\alpha\beta$  to effectively induce this effect ( $\leq 20\%$  stimulation of cGMP binding; data not shown). Full stimulation of cGMP binding by P $\gamma$  could be achieved if ten additional amino acids were present (P $\gamma$ 10–30) to help stabilize peptide binding to P $\alpha\beta$  ( $K_{1/2}$  of 10  $\mu$ M; Fig. 3B, see also Ref. (15)). Partial (47%) restoration of P $\gamma$ -mediated cGMP binding was observed with a peptide of intermediate length, P $\gamma$ 19–30, but with substantially lower peptide binding affinity ( $K_{1/2} = 280 \mu$ M; Fig. 3B). These results with P $\gamma$  synthetic peptides reveal for the first time that amino acid residues 10–18 within the N-terminal region of P $\gamma$  can play a local, stabilizing role in the ability of P $\gamma$  to stimulate cGMP binding to the GAF domains of P $\alpha\beta$ .

We conclude from these results that four amino acids (Pro27-Pro28-Lys29-Phe30) bordering the pro-rich and polycationic regions of P $\gamma$  are required to enhance cGMP binding affinity to the GAFa domains of P $\alpha\beta$ . Neighboring residues on

## Functional Interaction Sites of P $\gamma$ with PDE6 and Transducin

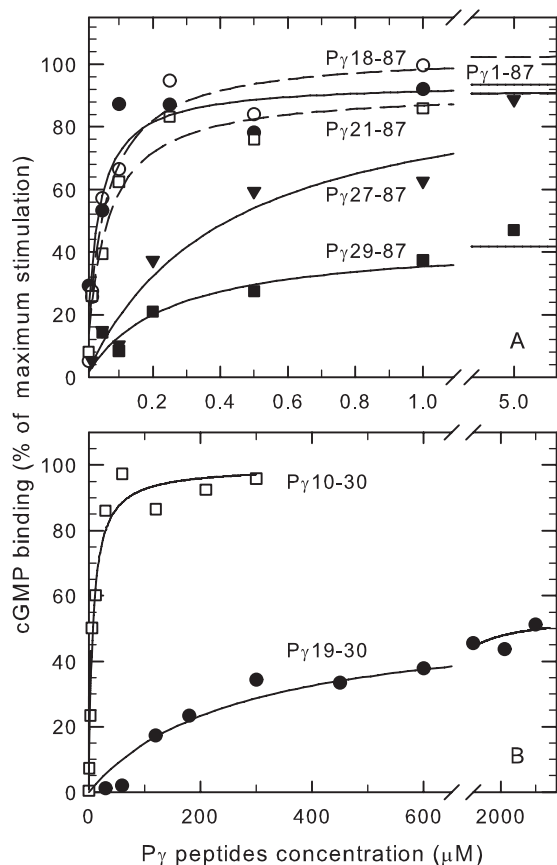


**FIGURE 3. Amino acids in the N-terminal portion of P $\gamma$  stabilize cGMP binding to the GAF domains of P $\alpha\beta$ .** Purified P $\alpha\beta$  (20 nM) was pre-incubated with 10 mM EDTA, 20 mM dipicolinic acid, and 50  $\mu$ M sildenafil for 2 h at 22 °C. [ $^3$ H]cGMP binding was measured in the presence of increasing amount of the indicated N-terminal truncated P $\gamma$  mutants (A) and synthetic peptides (B), and is reported as the percent stimulation of cGMP binding when comparing P $\alpha\beta$  (0% stimulation) to P $\alpha\beta$  incubated with 1  $\mu$ M wild-type P $\gamma$  (100% stimulation,  $B_{\max}$ ). The data are the average of at least three experiments, with the curves representing the fit of the data to a hyperbolic function. A, N-terminal truncated P $\gamma$  mutants: P $\gamma$ 1–87 (●),  $K_{1/2} = 31 \pm 10$  nM,  $B_{\max} = 94\%$ ; P $\gamma$ 18–87 (○),  $K_{1/2} = 52 \pm 13$  nM,  $B_{\max} = 104\%$ ; P $\gamma$ 21–87 (□),  $K_{1/2} = 56 \pm 11$  nM,  $B_{\max} = 91\%$ ; P $\gamma$ 27–87 (▼),  $K_{1/2} = 409 \pm 85$  nM,  $B_{\max} = 98\%$ ; P $\gamma$ 29–87 (■),  $K_{1/2} = 457 \pm 180$  nM,  $B_{\max} = 44\%$ . B, synthetic P $\gamma$  peptides: P $\gamma$ 10–30 (□),  $K_{1/2} = 10 \pm 4.3$   $\mu$ M,  $B_{\max} = 107\%$ ; P $\gamma$ 19–30 (●),  $K_{1/2} = 280 \pm 70$   $\mu$ M,  $B_{\max} = 47\%$ .

either side of this tetrapeptide provide local stabilizing interactions between P $\gamma$  and the P $\alpha\beta$  GAF domains that enhance the effectiveness of this four-amino acid segment, consistent with chemical cross-linking studies showing interactions of Val-21, Pro-23, and Phe-30 with the GAF domains of the PDE6 catalytic subunits (16, 17, 50).

**P $\gamma$  Residue Ile-54 Is Important for T $\alpha^*$ -GTP $\gamma$ S to Relieve Inhibition of PDE6 Catalysis**—Previous work demonstrated that activated transducin was incapable of relieving inhibition of catalysis resulting from binding of the C-terminal fragment (P $\gamma$ 63–87) reconstituted with P $\alpha\beta$ , suggesting that activated transducin required additional sites of interaction with P $\gamma$  to effectively de-inhibit PDE6 catalysis (10). To identify additional regions of P $\gamma$  responsible for the favorable interactions with T $\alpha^*$ -GTP $\gamma$ S leading to de-inhibition, we created a series of N-terminal truncation mutants that span the entire amino acid sequence of P $\gamma$ . These purified peptides were reconstituted with P $\alpha\beta$  at concentrations sufficient to inhibit catalysis by 80% or greater (Fig. 4, solid bars). As expected, a short truncation of

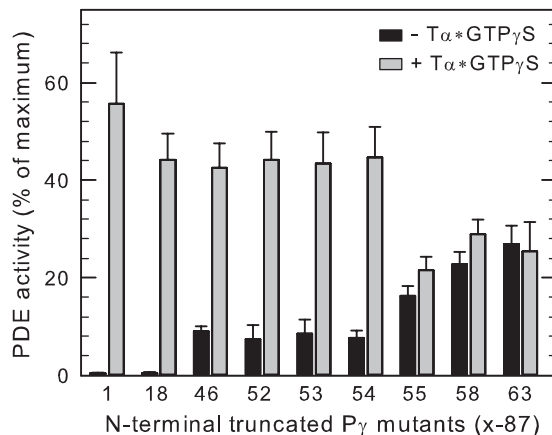


**FIGURE 4. Isoleucine-54 of P $\gamma$  is critical for transducin to effectively bind to P $\gamma$  to relieve inhibition of catalysis.** Purified P $\alpha\beta$  (1 nM) was incubated with the indicated N-terminal truncated P $\gamma$  mutants (x-87, where x is the first amino acid position number) to suppress 80% or greater of the catalytic activity: 5 nM P $\gamma$ 1–87; 10 nM P $\gamma$ 18–87; 0.5  $\mu$ M P $\gamma$ 46–87; 1  $\mu$ M P $\gamma$ 52–87; and P $\gamma$ 53–87; 2  $\mu$ M P $\gamma$ 54–87; 5  $\mu$ M P $\gamma$ 55–87; and P $\gamma$ 58–87; data for P $\gamma$ 63–87 was taken from Ref. 10. Following 10 min of incubation at room temperature, activated transducin (10  $\mu$ M) was added to one portion of each reconstituted PDE6 preparation, followed by addition of 2 mM cGMP to measure PDE6 catalytic activity. The data are the mean  $\pm$  S.E. for three individual experiments and are reported as the percent of P $\alpha\beta$  activity when no additional P $\gamma$  was present.

the N-terminal region (P $\gamma$ 18–87) that retains the GAF-interacting domain of P $\gamma$  was capable of effectively interacting with T $\alpha^*$ -GTP $\gamma$ S to relieve inhibition of PDE6 catalysis (Fig. 4, gray bars). Unexpectedly, when P $\alpha\beta$  was reconstituted with P $\gamma$ 46–87 (which lacks the entire GAF-interacting region), addition of activated transducin resulted in activation of PDE6 catalysis (Fig. 4). This demonstrates that the GAF interacting region of P $\gamma$  is not a requirement for transducin activation of PDE6. Transducin also successfully de-inhibited P $\alpha\beta$  reconstituted with P $\gamma$ 52–87, P $\gamma$ 53–87, and P $\gamma$ 54–87 to the same maximum extent as wild type P $\gamma$ . However, P $\alpha\beta$  reconstituted with P $\gamma$ 55–87 was unable to be fully activated by T $\alpha^*$ -GTP $\gamma$ S, and shorter peptides (e.g. P $\gamma$ 58–87) were also ineffective (<10% activation, Fig. 4). We conclude that Ile54 in the glycine-rich region of P $\gamma$  is essential for transducin to effectively interact with P $\gamma$  to displace the C-terminal region to fully activate PDE6 catalysis.

Ile54 of P $\gamma$  has been visualized in proximity to the Trp-70 residue (important in the ability of T $\alpha^*$  to activate PDE6) in the crystal structure of a complex of a C-terminal P $\gamma$  fragment, a chimeric form of transducin  $\alpha$ -subunit, and the RGS domain of RGS9–1 (23). Chemical cross-linking studies have shown much more favorable interactions of the glycine-rich region of P $\gamma$  with PDE6 catalytic subunits compared with transducin (26). Together with our work, these results support the hypothesis that the glycine-rich region of P $\gamma$  plays a critical role in the transducin activation mechanism of PDE6. We propose that in the transition from the dark-adapted to light-activated state, the glycine-rich region of P $\gamma$  relays its interactions from the P $\alpha\beta$  catalytic dimer to T $\alpha^*$  as it binds to the PDE6 holoenzyme. This “docking” of T $\alpha^*$  to the glycine-rich region of P $\gamma$  (centering around Ile-54) is necessary for T $\alpha^*$  to form additional interactions with the C-terminal region of P $\gamma$  (to displace the C-terminal region of P $\gamma$  from its binding sites in the catalytic pocket

to de-inhibit catalysis) as well as the N-terminal half of P $\gamma$  (see next section).

**Interaction of T $\alpha^*$ -GTP $\gamma$ S with the Glycine-rich Region of P $\gamma$  Increases the Rate of cGMP Dissociation from PDE6 GAFa Domains**—The region of P $\gamma$  that stabilizes cGMP binding to the GAFa domains of P $\alpha\beta$  (amino acids 21 to 30; see above) have also been reported to interact with transducin  $\alpha$ -subunit based on binding assays of P $\gamma$ 21–45 with T $\alpha^*$ -GTP $\gamma$ S (28, 29). To directly test whether T $\alpha^*$ -GTP $\gamma$ S can alter cGMP binding to the GAFa domain through disrupting P $\gamma$  binding to P $\alpha\beta$ , we measured the ability of T $\alpha^*$ -GTP $\gamma$ S to accelerate the rate of cGMP dissociation from P $\alpha\beta$  reconstituted with various P $\gamma$  fragments. As shown in Fig. 5A, addition of T $\alpha^*$ -GTP $\gamma$ S to P $\alpha\beta$  reconstituted with full-length P $\gamma$  increased  $2.2 \pm 0.2$ -fold ( $n = 4$ ) the rate at which cGMP exchange occurs at the noncatalytic cGMP binding sites. P $\gamma$ 1–60 was equally effective ( $2.2 \pm 0.4$ -fold;  $n = 3$ ) as wild-type in this regard (Fig. 5B). In contrast, P $\gamma$ 1–45 reconstituted with P $\alpha\beta$  showed virtually no stimulation of cGMP dissociation rate ( $1.2 \pm 0.1$ -fold;  $n = 5$ ) upon T $\alpha^*$ -GTP $\gamma$ S addition (Fig. 5C). We conclude that T $\alpha^*$ -GTP $\gamma$ S requires interactions with P $\gamma$  in the glycine-rich region (specifically amino acids 46–60) in order to weaken the interactions of P $\gamma$  in the region of amino acids 21–30 that are responsible for modulating cGMP affinity to the GAFa domains of PDE6. The ability of activated transducin  $\alpha$ -subunit to accelerate cGMP dissociation may represent a negative feedback mechanism operating during light adaptation (see “Conclusions”).

**Characterization of the Regions of P $\gamma$  Important for Facilitating Deactivation of the Complex of PDE6/Transducin/RGS9–1**—Another important role of P $\gamma$  is to form a protein complex with RGS9–1, transducin, and other accessory proteins to accelerate the GTPase activity of activated transducin during deactivation of PDE6 (38). However, there is conflicting evidence regarding the sites of interaction of P $\gamma$  with this complex (see Introduction). To precisely define the P $\gamma$  residues required for GTPase acceleration, we first utilized a set of P $\gamma$  mutants truncated to various extents at the C terminus. These P $\gamma$  mutants were incubated with ROS membranes and tested for their ability to accelerate the GTPase activity of transducin above the intrinsic activity of this membrane preparation. As shown in Fig. 6A, wild-type P $\gamma$  (P $\gamma$ 1–87) and a mutant lacking the terminal Ile-87 (P $\gamma$ 1–86) both stimulated the GTPase rate by  $\sim 2.5$ -fold compared with the control lacking any exogenous P $\gamma$ . Removal of an additional amino acid (P $\gamma$ 1–85) slowed the GTPase rate by 60% compared with full-length P $\gamma$ , consistent with a previous study (20). We conclude that a single amino acid, Ile-86, is critical for the ability of P $\gamma$  to potentiate GTPase acceleration.

Larger C-terminal truncations of P $\gamma$  (e.g. P $\gamma$ 1–70 (not shown) or P $\gamma$ 1–45 (Fig. 6A)) caused no further disruption of its ability to stimulate the GTPase rate. To determine the potential participation of the N-terminal half of P $\gamma$  in GTPase acceleration, we tested the ability of P $\gamma$ 46–87 to accelerate GTPase activity. We found a modest (2-fold) decrease in overall affinity of P $\gamma$ 46–87 with the transducin/RGS9–1 complex ( $K_{1/2} = 0.35 \pm 0.04 \mu\text{M}$ ) compared with wild-type P $\gamma$  ( $K_{1/2} = 0.14 \pm 0.02 \mu\text{M}$ ). This indicates no significant role for the N-terminal

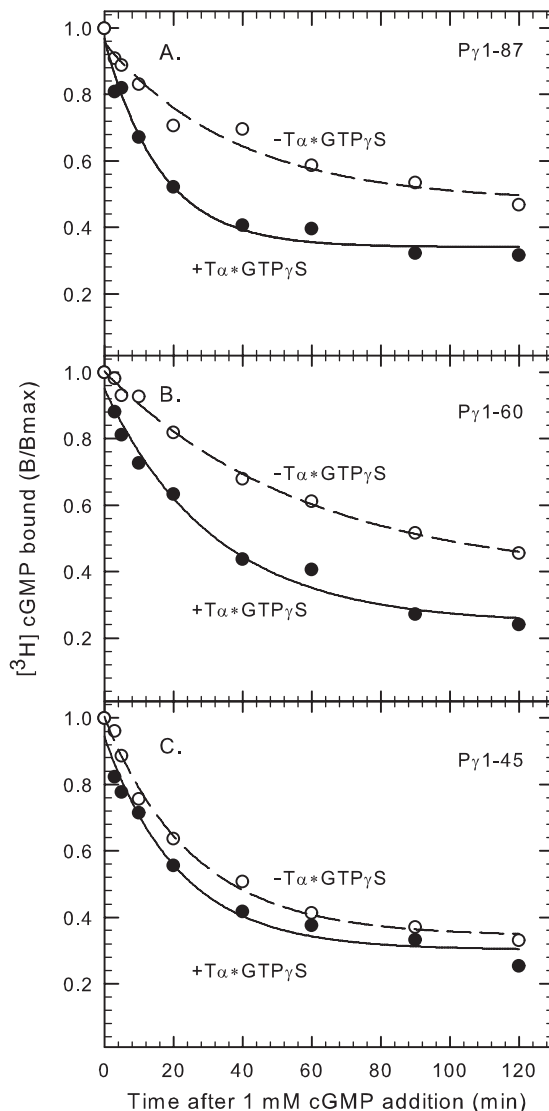


**FIGURE 5. Interaction of transducin with the glycine-rich region of P $\gamma$  increases the rate of cGMP dissociation from PDE6.** Nucleotide-depleted P $\alpha\beta$  (20 nM) was pre-incubated with 10 mM EDTA, 20 mM dipicolinic acid, and 50  $\mu\text{M}$  vardenafil for 2 h at 22 °C. [ $^3\text{H}$ ]cGMP was added in the presence of 40–80 nM full-length P $\gamma$  (A), P $\gamma$ 1–60 (B), or P $\gamma$ 1–45 (C), and the samples incubated for 5 min. For each condition, addition of P $\gamma$  or truncated mutants stimulated binding 1.5-fold compared with P $\alpha\beta$  dimer alone; the maximum extent of binding ( $B_{\text{max}}$ ) just prior to initiating dissociation was P $\gamma$ 1–87,  $1.7 \pm 0.2$  mol cGMP/mol P $\alpha\beta$ ; P $\gamma$ 1–60,  $1.7 \pm 0.1$  mol cGMP/mol P $\alpha\beta$ ; P $\gamma$ 1–45,  $1.6 \pm 0.1$  mol cGMP/mol P $\alpha\beta$ . [ $^3\text{H}$ ]cGMP dissociation was induced by addition of unlabeled cGMP supplemented with or without 2  $\mu\text{M}$  activated transducin (T $\alpha^*$ -GTP $\gamma$ S), and the amount bound (B) assayed at various times thereafter. The data shown in the figure are from one representative experiment, with the results fitted to a single-exponential decay process with  $t_{1/2}$  values as follows: A,  $-T\alpha^* = 26.3$  min,  $+T\alpha^* = 11.2$  min; B,  $-T\alpha^* = 40.5$  min,  $+T\alpha^* = 22.1$  min; C,  $-T\alpha^* = 17.7$  min,  $+T\alpha^* = 15.0$  min.

half of P $\gamma$  to participate in GTPase acceleration in the T $\alpha^*$ -GTP $\gamma$ S/RGS9–1 complex.

To identify more precisely which regions of P $\gamma$  interact with the transducin/RGS9–1 complex to stimulate GTPase activity, we next tested the ability of C-terminal synthetic peptides and N-terminal truncation mutants of P $\gamma$  to maximally accelerate the GTPase activity of ROS membrane preparations. We first determined that P $\gamma$ 65–87 was the minimum C-terminal fragment sufficient to cause maximal stimulation of GTPase activ-

## Functional Interaction Sites of P $\gamma$ with PDE6 and Transducin

ity, since removal of two additional amino acids (P $\gamma$ 67–87) abolished the potentiating effect entirely (Fig. 6B). To quantitatively define the regions of P $\gamma$  that enhance its effectiveness to accelerate GTPase activity, we examined the concentration dependence of this acceleration effect. Whereas P $\gamma$ 67–87 was

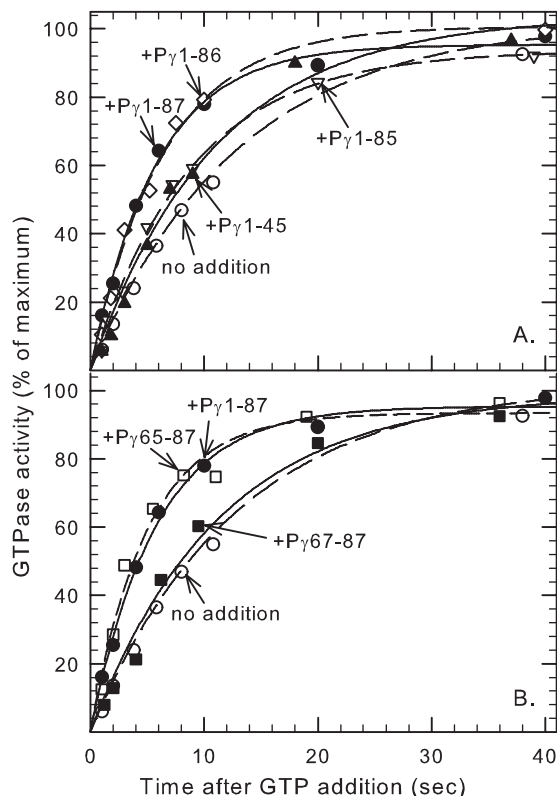


**FIGURE 6. Two major regions of P $\gamma$  are critical for the acceleration of GTPase activity of activated transducin.** Bovine ROS membranes (containing PDE6, transducin, and RGS9–1) were incubated with P $\gamma$  truncation mutants for 20 min at room temperature. GTPase activity was then measured by addition of 0.1  $\mu$ M [ $\gamma$ - $^{32}$ P]GTP. The reaction was stopped at the indicated time by addition of perchloric acid. GTPase activity is reported as a percent of maximum activity (1 h incubation; >98% substrate hydrolyzed). The data shown in the figure are representative of at least three different experiments, in which the lines represent the fit of the data to a single exponential rise to maximum. **A**, C-terminal truncated P $\gamma$  mutants (2  $\mu$ M final concentration): no addition ( $\circ$ ),  $t_{1/2} = 8.0 \pm 0.8$  s; P $\gamma$ 1–45 ( $\blacktriangle$ ),  $t_{1/2} = 6.2 \pm 0.9$  s; P $\gamma$ 1–85 ( $\nabla$ ),  $t_{1/2} = 5.7 \pm 0.7$  s; P $\gamma$ 1–86 ( $\diamond$ ),  $t_{1/2} = 3.7 \pm 0.4$  s; P $\gamma$ 1–87 ( $\bullet$ ),  $t_{1/2} = 3.1 \pm 0.8$  s. **B**, N-terminal truncation mutants of P $\gamma$  (tested at 10  $\mu$ M final concentration): no addition ( $\circ$ ),  $t_{1/2} = 8.0 \pm 0.8$  s; P $\gamma$ 65–87 ( $\square$ ),  $t_{1/2} = 3.1 \pm 0.3$  s; and P $\gamma$ 67–87 ( $\blacksquare$ ),  $t_{1/2} = 6.8 \pm 0.4$  s. In all cases except for P $\gamma$ 67–87, the  $t_{1/2}$  values for the indicated P $\gamma$  mutants were statistically significant ( $p < 0.01$ ) compared with the control (no P $\gamma$  added).

completely ineffective at highest concentrations tested (500  $\mu$ M), adding Thr-65 and Val-66 enhanced >100-fold the ability of P $\gamma$  to potentiate the GTPase activity of the transducin/RGS9–1 complex (P $\gamma$ 65–87,  $K_{1/2} = 2.5 \pm 1.4$   $\mu$ M). Addition of two more amino acids (P $\gamma$ 63–87;  $K_{1/2} = 2.2 \pm 0.3$   $\mu$ M) had no effect on the affinity, while inclusion of an additional eight amino acids (P $\gamma$ 55–87;  $K_{1/2} = 0.6 \pm 0.2$   $\mu$ M) stabilized the interaction 4-fold. Further elongation of P $\gamma$  had little effect on the ability to stimulate GTPase activity.

Two conclusions arise from these results: 1) Ile-86 in conjunction with Thr-65 and/or Val-66 of P $\gamma$  are required to maximally accelerate the GTPase rate of the T $\alpha^*$ /RGS9–1 complex, consistent with previous evidence (20, 23); 2) stabilizing interactions in the region of amino acids 55–62 of P $\gamma$  may help anchor P $\gamma$  to the T $\alpha^*$ /RGS9–1 complex even though they are not required for maximal potentiation of the GTPase rate.

## CONCLUSIONS

This comprehensive analysis of the functionally important regions of the inhibitory  $\gamma$ -subunit that interact with the PDE6 catalytic dimer, with activated transducin  $\alpha$ -subunit, and with the T $\alpha^*$ /RGS9–1 complex (summarized in Fig. 7) reveals the complexity of the regulatory mechanisms mediated by multiple regions of this small protein. The ability of the N-terminal and C-terminal regions of P $\gamma$  to span the surface of the P $\alpha\beta$  dimer from the GAFa domain to the active site of the catalytic domain underscores the extended linear structure that P $\gamma$  must assume when associated with the P $\alpha\beta$  catalytic dimer. Since P $\gamma$  free in solution is a natively unfolded protein (6, 51, 52), its extended conformation is a consequence of binding to the P $\alpha\beta$  dimer at each of the six distinct regions of the P $\gamma$  linear structure (defined in Fig. 7). Because P $\gamma$  seldom (if ever) completely dissociates from P $\alpha\beta$  during mammalian visual transduction (53–55), it is likely that the structural elements important for interaction of P $\gamma$  with T $\alpha^*$ , RGS9–1, or other putative binding partners (e.g. GARP2 (56)) occur while P $\gamma$  is associated with the catalytic subunits and involve a disruption of P $\gamma$ -P $\alpha\beta$  interactions at the same time as new interactions form between P $\gamma$  and its other binding partners.

Our work reveals the central importance of the glycine-rich region of P $\gamma$  as a primary “docking site” with P $\alpha\beta$  (amino acids 52–54), with T $\alpha^*$  (amino acids 54–55), and with the T $\alpha^*$ /RGS9–1 complex (amino acids 55–62; Fig. 7). We hypothesize that this stretch of amino acids stabilizes binding of T $\alpha^*$  to

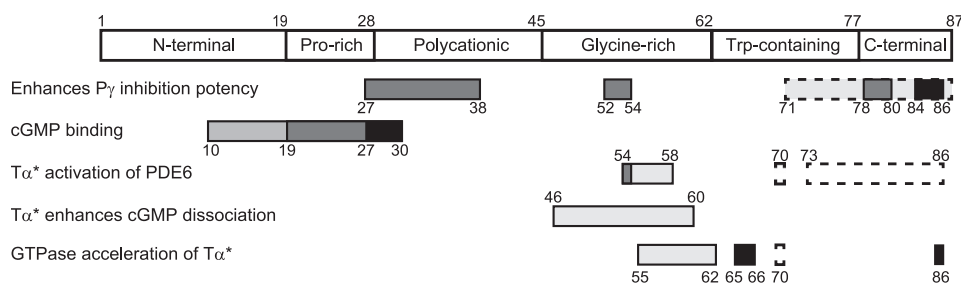


**FIGURE 7. Functionally important interaction sites of the inhibitory P $\gamma$  subunit with PDE6, transducin, and the transducin/RGS9–1 complex.** The 87 amino acid P $\gamma$  subunit is defined in terms of six structurally distinct domains: N-terminal region (amino acids 1–19); proline-rich region (amino acids 20–28); polycationic region (amino acids 29–45); glycine-rich region (amino acids 46–62); tryptophan-containing region (amino acids 63–77); and the C-terminal region (amino acids 78–87). The sites that are required for any of the five given functions are shown with *solid black boxes*. Amino acid residues having major stabilizing effects on P $\gamma$  binding to its binding partner are shown in *dark gray*, while additional, weaker sites of interaction are shown in *light gray*. The *dashed boxes* represent critical functional regions of P $\gamma$  identified previously (10, 20, 22, 24).

position it to develop additional interactions with the C-terminal “hinge” (amino acids 71–77) and “blocking” (amino acids 78–87) regions of P $\gamma$  (8, 24) that lead to de-inhibition of PDE6 catalysis. A subset of residues within the glycine-rich region of P $\gamma$  (specifically amino acids 55–62) is also implicated in facilitating the potentiating role of P $\gamma$  to accelerate GTPase activity of the T $\alpha^*$ /RGS9–1 complex. Further, this same region of P $\gamma$  is implicated in regulating cGMP exchange kinetics at the non-catalytic cGMP binding sites of P $\alpha\beta$ . This latter effect may result from another hinge-like mechanism whereby docking of T $\alpha^*$  to the glycine-rich region of P $\gamma$  enables T $\alpha^*$  to form additional, previously identified, interactions with the polycationic region of P $\gamma$  (27–30) which could, in turn, counteract the stabilizing effects of the Pro-rich region (amino acids 27–30) of P $\gamma$  on cGMP binding to the GAF $\alpha$  domains of P $\alpha\beta$ .

These multiple interactions of P $\gamma$  with P $\alpha\beta$  and with other PDE6 binding partners likely occur in an exquisitely controlled temporal sequence that begins with the immediate response to light stimulation of a dark-adapted photoreceptor (*i.e.* visual excitation leading to PDE6 activation by T $\alpha^*$ ). This leads to the subsequent acceleration of photoresponse recovery during light adaptation (RGS9–1-catalyzed acceleration of T $\alpha^*$  GTPase activity being the rate-limiting step; (32)). Finally, slowly developing aspects of photoreceptor desensitization (reviewed in Ref. (2)) may relate to the ability of T $\alpha^*$ -activated PDE6 to increase cGMP dissociation from noncatalytic cGMP binding sites on PDE6 when cytosolic cGMP levels remain low for an extended time. All of these above-mentioned interactions are mediated by changes in P $\gamma$  interactions with P $\alpha\beta$ , T $\alpha^*$ , RGS9–1, and other proteins that form a large multiprotein signaling complex on the photoreceptor disk membrane (57). Future efforts will be directed to mapping the individual regions of P $\gamma$  that serve to relay information about the state of light activation from P $\alpha\beta$  to the other members of this signaling complex, furthering our understanding of the mechanistic basis for visual dysfunction and photoreceptor degeneration that can result from genetic defects in P $\gamma$  or its binding partners (4).

*Acknowledgments*—We thank Sue Matte, Karyn Cahill, and Christina Loporcaro for help with construction of some of the P $\gamma$  mutants, protein purification, and manuscript review.

## REFERENCES

- Cote, R. H. (2006) in Photoreceptor phosphodiesterase (PDE6): a G-protein-activated PDE regulating visual excitation in rod and cone photoreceptor cells. (Beavo, J. A., Francis, S. H., and Houslay, M. D., eds) *Cyclic Nucleotide Phosphodiesterases in Health and Disease*, pp. 165–193, CRC Press, Boca Raton, FL
- Arshavsky, V. Y., and Burns, M. E. (2012) Photoreceptor signaling: supporting vision across a wide range of light intensities. *J. Biol. Chem.* **287**, 1620–1626
- Daiger, S. P., Bowne, S. J., and Sullivan, L. S. (2007) Perspective on genes and mutations causing retinitis pigmentosa. *Arch. Ophthalmol.* **125**, 151–158
- Baehr, W., and Frederick, J. M. (2009) Naturally occurring animal models with outer retina phenotypes. *Vision Res.* **49**, 2636–2652
- Ferrari, S., Di Iorio, E., Barbaro, V., Ponzin, D., Sorrentino, F. S., and Parmeggiani, F. (2011) Retinitis pigmentosa: genes and disease mechanisms. *Curr. Genomics* **12**, 238–249
- Guo, L. W., and Ruoho, A. E. (2008) The retinal cGMP phosphodiesterase  $\gamma$ -subunit - a chameleon. *Curr. Protein Pept. Sci.* **9**, 611–625
- Granovsky, A. E., Natochin, M., and Artemyev, N. O. (1997) The  $\gamma$ -subunit of rod cGMP-phosphodiesterase blocks the enzyme catalytic site. *J. Biol. Chem.* **272**, 11686–11689
- Barren, B., Gakhar, L., Muradov, H., Boyd, K. K., Ramaswamy, S., and Artemyev, N. O. (2009) Structural basis of phosphodiesterase 6 inhibition by the C-terminal region of the  $\gamma$ -subunit. *EMBO J.* **28**, 3613–3622
- Zhang, Z., and Artemyev, N. O. (2010) Determinants for phosphodiesterase 6 inhibition by its  $\gamma$ -subunit. *Biochemistry* **49**, 3862–3867
- Zhang, X. J., Skiba, N. P., and Cote, R. H. (2010) Structural requirements of the photoreceptor phosphodiesterase  $\gamma$ -subunit for inhibition of rod PDE6 holoenzyme and for its activation by transducin. *J. Biol. Chem.* **285**, 4455–4463
- Yamazaki, A., Bartucca, F., Ting, A., and Bitensky, M. W. (1982) Reciprocal effects of an inhibitory factor on catalytic activity and noncatalytic cGMP binding sites of rod phosphodiesterase. *Proc. Natl. Acad. Sci. U.S.A.* **79**, 3702–3706
- Cote, R. H., Bownds, M. D., and Arshavsky, V. Y. (1994) cGMP binding sites on photoreceptor phosphodiesterase: role in feedback regulation of visual transduction. *Proc. Natl. Acad. Sci. U.S.A.* **91**, 4845–4849
- Artemyev, N. O., and Hamm, H. E. (1992) Two-site high-affinity interaction between inhibitory and catalytic subunits of rod cyclic GMP phosphodiesterase. *Biochem. J.* **283**, 273–279
- Takemoto, D. J., Hurt, D., Oppert, B., and Cunnick, J. (1992) Domain mapping of the retinal cyclic GMP phosphodiesterase  $\gamma$ -subunit. Function of the domains encoded by the three exons of the  $\gamma$ -subunit gene. *Biochem. J.* **281**, 637–643
- Mou, H., and Cote, R. H. (2001) The catalytic and GAF domains of the rod cGMP phosphodiesterase (PDE6) heterodimer are regulated by distinct regions of its inhibitory  $\gamma$ -subunit. *J. Biol. Chem.* **276**, 27527–27534
- Guo, L. W., Grant, J. E., Hajipour, A. R., Muradov, H., Arbaban, M., Artemyev, N. O., and Ruoho, A. E. (2005) Asymmetric interaction between rod cyclic GMP phosphodiesterase  $\gamma$ -subunits and  $\alpha\beta$ -subunits. *J. Biol. Chem.* **280**, 12585–12592
- Guo, L. W., Muradov, H., Hajipour, A. R., Sievert, M. K., Artemyev, N. O., and Ruoho, A. E. (2006) The inhibitory  $\gamma$ -subunit of the rod cGMP phosphodiesterase binds the catalytic subunits in an extended linear structure. *J. Biol. Chem.* **281**, 15412–15422
- Aravind, L., and Ponting, C. P. (1997) The GAF domain: an evolutionary link between diverse phototransducing proteins. *Trends Biochem. Sci.* **22**, 458–459
- Skiba, N. P., Artemyev, N. O., and Hamm, H. E. (1995) The carboxyl terminus of the gamma-subunit of rod cGMP phosphodiesterase contains distinct sites of interaction with the enzyme catalytic subunits and the  $\alpha$ -subunit of transducin. *J. Biol. Chem.* **270**, 13210–13215
- Slepek, V. Z., Artemyev, N. O., Zhu, Y., Dumke, C. L., Sabacan, L., Sondak, J., Hamm, H. E., Bownds, M. D., and Arshavsky, V. Y. (1995) An effector site that stimulates G-protein GTPase in photoreceptors. *J. Biol. Chem.* **270**, 14319–14324
- Liu, Y., Arshavsky, V. Y., and Ruoho, A. E. (1996) Interaction sites of the COOH-terminal region of the  $\gamma$ -subunit of cGMP phosphodiesterase with the GTP-bound  $\alpha$ -subunit of transducin. *J. Biol. Chem.* **271**, 26900–26907
- Tsang, S. H., Burns, M. E., Calvert, P. D., Gouras, P., Baylor, D. A., Goff, S. P., and Arshavsky, V. Y. (1998) Role for the target enzyme in deactivation of photoreceptor G protein *in vivo*. *Science* **282**, 117–121
- Slep, K. C., Kercher, M. A., He, W., Cowan, C. W., Wensel, T. G., and Sigler, P. B. (2001) Structural determinants for regulation of phosphodiesterase by a G protein at 2.0 Å. *Nature* **409**, 1071–1077
- Granovsky, A. E., and Artemyev, N. O. (2001) A conformational switch in the inhibitory gamma-subunit of PDE6 upon enzyme activation by transducin. *Biochemistry* **40**, 13209–13215
- Grant, J. E., Guo, L. W., Vestling, M. M., Martemyanov, K. A., Arshavsky, V. Y., and Ruoho, A. E. (2006) The N terminus of GTP  $\gamma$ S-activated transducin  $\alpha$ -subunit interacts with the C terminus of the cGMP phosphodiesterase  $\gamma$ -subunit. *J. Biol. Chem.* **281**, 6194–6202
- Guo, L. W., Hajipour, A. R., and Ruoho, A. E. (2010) Complementary interactions of the rod PDE6 inhibitory subunit with the catalytic subunits



## Functional Interaction Sites of P $\gamma$ with PDE6 and Transducin

- and transducin. *J. Biol. Chem.* **285**, 15209–15219
27. Morrison, D. F., Cunnick, J. M., Oppert, B., and Takemoto, D. J. (1989) Interaction of the gamma-subunit of retinal rod outer segment phosphodiesterase with transducin. Use of synthetic peptides as functional probes. *J. Biol. Chem.* **264**, 11671–11681
  28. Artemyev, N. O., Rarick, H. M., Mills, J. S., Skiba, N. P., and Hamm, H. E. (1992) Sites of interaction between rod G-protein  $\alpha$ -subunit and cGMP-phosphodiesterase  $\gamma$ -subunit. Implications for the phosphodiesterase activation mechanism. *J. Biol. Chem.* **267**, 25067–25072
  29. Artemyev, N. O., Mills, J. S., Thornburg, K. R., Knapp, D. R., Schey, K. L., and Hamm, H. E. (1993) A site on transducin  $\alpha$ -subunit of interaction with the polycationic region of cGMP phosphodiesterase inhibitory subunit. *J. Biol. Chem.* **268**, 23611–23615
  30. Artemyev, N. O. (1997) Binding of transducin to light-activated rhodopsin prevents transducin interaction with the rod cGMP phosphodiesterase  $\gamma$ -subunit. *Biochemistry* **36**, 4188–4193
  31. Muradov, H., Boyd, K. K., and Artemyev, N. O. (2010) Rod phosphodiesterase-6 PDE6A and PDE6B subunits are enzymatically equivalent. *J. Biol. Chem.* **285**, 39828–39834
  32. Krispel, C. M., Chen, D., Melling, N., Chen, Y. J., Martemyanov, K. A., Quillinan, N., Arshavsky, V. Y., Wensel, T. G., Chen, C. K., and Burns, M. E. (2006) RGS expression rate-limits recovery of rod photoresponses. *Neuron* **51**, 409–416
  33. Anderson, G. R., Posokhova, E., and Martemyanov, K. A. (2009) The R7 RGS protein family: multi-subunit regulators of neuronal G protein signaling. *Cell Biochem. Biophys.* **54**, 33–46
  34. He, W., Cowan, C. W., and Wensel, T. G. (1998) RGS9, a GTPase accelerator for phototransduction. *Neuron* **20**, 95–102
  35. Makino, E. R., Handy, J. W., Li, T., and Arshavsky, V. Y. (1999) The GTPase activating factor for transducin in rod photoreceptors is the complex between RGS9 and type 5 G protein  $\beta$ -subunit. *Proc. Natl. Acad. Sci. U.S.A.* **96**, 1947–1952
  36. Skiba, N. P., Hopp, J. A., and Arshavsky, V. Y. (2000) The effector enzyme regulates the duration of G protein signaling in vertebrate photoreceptors by increasing the affinity between transducin and RGS protein. *J. Biol. Chem.* **275**, 32716–32720
  37. Hu, G., and Wensel, T. G. (2002) R9AP, a membrane anchor for the photoreceptor GTPase accelerating protein, RGS9-1. *Proc. Natl. Acad. Sci. U.S.A.* **99**, 9755–9760
  38. Arshavsky, V. Y., Dumke, C. L., Zhu, Y., Artemyev, N. O., Skiba, N. P., Hamm, H. E., and Bownds, M. D. (1994) Regulation of transducin GTPase activity in bovine rod outer segments. *J. Biol. Chem.* **269**, 19882–19887
  39. Guo, L. W., and Ruoho, A. E. (2011) N-terminal half of the cGMP phosphodiesterase  $\gamma$ -subunit contributes to stabilization of the GTPase-accelerating protein complex. *J. Biol. Chem.* **286**, 15260–15267
  40. Woodruff, M. L., Janisch, K. M., Peshenko, I. V., Dizhoor, A. M., Tsang, S. H., and Fain, G. L. (2008) Modulation of phosphodiesterase6 turnover during background illumination in mouse rod photoreceptors. *J. Neurosci.* **28**, 2064–2074
  41. Smith, P. K., Krohn, R. I., Hermanson, G. T., Mallia, A. K., Gartner, F. H., Provenzano, M. D., Fujimoto, E. K., Goeke, N. M., Olson, B. J., and Klenk, D. C. (1985) Measurement of protein using bicinchoninic acid. *Anal. Biochem.* **150**, 76–85
  42. Pentia, D. C., Hosier, S., Collupy, R. A., Valeriani, B. A., and Cote, R. H. (2005) Purification of PDE6 isozymes from mammalian retina. *Methods Mol. Biol.* **307**, 125–140
  43. Cote, R. H. (2000) Kinetics and regulation of cGMP binding to noncatalytic binding sites on photoreceptor phosphodiesterase. *Methods Enzymol.* **315**, 646–672
  44. Mou, H., Grazio, H. J., 3rd, Cook, T. A., Beavo, J. A., and Cote, R. H. (1999) cGMP binding to noncatalytic sites on mammalian rod photoreceptor phosphodiesterase is regulated by binding of its  $\gamma$ - and  $\delta$ -subunits. *J. Biol. Chem.* **274**, 18813–18820
  45. Hurley, J. B., and Stryer, L. (1982) Purification and characterization of the  $\gamma$  regulatory subunit of the cyclic GMP phosphodiesterase from retinal rod outer segments. *J. Biol. Chem.* **257**, 11094–11099
  46. Cote, R. H. (2005) Cyclic guanosine 5'-monophosphate binding to regulatory GAF domains of photoreceptor phosphodiesterase. *Methods Mol. Biol.* **307**, 141–154
  47. Cowan, C. W., Wensel, T. G., and Arshavsky, V. Y. (2000) Enzymology of GTPase acceleration in phototransduction. *Methods Enzymol.* **315**, 524–538
  48. Kleuss, C., Pallast, M., Brendel, S., Rosenthal, W., and Schultz, G. (1987) Resolution of transducin subunits by chromatography on blue Sepharose. *J. Chromatogr.* **407**, 281–289
  49. Wensel, T. G., He, F., and Malinski, J. A. (2005) Purification, reconstitution on lipid vesicles, and assays of PDE6 and its activator G protein, transducin. *Methods Mol. Biol.* **307**, 289–313
  50. Muradov, K. G., Granovsky, A. E., Schey, K. L., and Artemyev, N. O. (2002) Direct interaction of the inhibitory  $\gamma$ -subunit of Rod cGMP phosphodiesterase (PDE6) with the PDE6 GAFa domains. *Biochemistry* **41**, 3884–3890
  51. Uversky, V. N., Permyakov, S. E., Zagranichny, V. E., Rodionov, I. L., Fink, A. L., Cherskaya, A. M., Wasserman, L. A., and Permyakov, E. A. (2002) Effect of zinc and temperature on the conformation of the  $\gamma$ -subunit of retinal phosphodiesterase: a natively unfolded protein. *J. Proteome Res.* **1**, 149–159
  52. Matte, S. L., Laue, T. M., and Cote, R. H. (2012) Characterization of conformational changes and protein-protein interactions of rod photoreceptor phosphodiesterase (PDE6). *J. Biol. Chem.* **287**, 20111–20121
  53. Wensel, T. G., and Stryer, L. (1986) Reciprocal control of retinal rod cyclic GMP phosphodiesterase by its  $\gamma$ -subunit and transducin. *Proteins* **1**, 90–99
  54. Deterre, P., Bigay, J., Robert, M., Pfister, C., Kühn, H., and Chabre, M. (1986) Activation of retinal rod cyclic GMP-phosphodiesterase by transducin: characterization of the complex formed by phosphodiesterase inhibitor and transducin  $\alpha$ -subunit. *Proteins* **1**, 188–193
  55. Otto-Bruc, A., Antonny, B., Vuong, T. M., Chardin, P., and Chabre, M. (1993) Interaction between the retinal cyclic GMP phosphodiesterase inhibitor and transducin. Kinetics and affinity studies. *Biochemistry* **32**, 8636–8645
  56. Pentia, D. C., Hosier, S., and Cote, R. H. (2006) The glutamic acid-rich protein-2 (GARP2) is a high affinity rod photoreceptor phosphodiesterase (PDE6)-binding protein that modulates its catalytic properties. *J. Biol. Chem.* **281**, 5500–5505
  57. Wensel, T. G. (2008) Signal transducing membrane complexes of photoreceptor outer segments. *Vision Res.* **48**, 2052–2061